Journal of Bone Oncology 16 (2019) 100220

Contents lists available at ScienceDirect

Journal of Bone Oncology

journal homepage: www.elsevier.com/locate/jbo

Research Paper

Novel 3D-printed prosthetic composite for reconstruction of massive bone defects in lower extremities after malignant tumor resection☆

Lu Yajie[a], Chen Guojing[a], Long Zuoyao[a], Li Minghui[a], Ji Chuanlei[a], Wang Fengwei[b], Li Huanzhang[a], Lu Jianxi[c], Wang Zhen[a,*], Li Jing[a,*]

[a] Department of Orthopedics, Xijing Hospital, The Air Force Medical University, No. 127 Changle West Road, Xi'an, Shaanxi 710032, PR China
[b] Department of Orthopedics, Shaanxi Zheng He Hospital, Xi'an, Shaanxi 710043, PR China
[c] Shanghai Bio-lu Biomaterials Co., Ltd., Shanghai 201100, PR China

ARTICLE INFO

Keywords:
3D printing
Prosthesis
Lower extremity
Reconstruction
Malignant tumor

ABSTRACT

Objective: To introduce a novel 3D-printed prosthetic composite for reconstruction of massive bone defects after resection for bone malignancy of lower extremities. The design concept, surgical technique, and the preliminary outcomes were elaborated.

Methods: Patients with primary malignant tumors of lower extremities requiring tumor resection and reconstruction were recruited between Jun 2015 and Nov 2018. Patient-specific 3D-printed prostheses were designed according to preoperative imaging data. After tumor resection, reconstruction was performed with composites consisting of 3D- printed prosthesis, beta-tricalcium phosphate (β-TCP) bioceramics and/or vascularized fibula. All patients underwent regular follow-up postoperatively. The functional outcomes were assessed by the Musculoskeletal Tumor Society score (MSTS). Oncological outcomes, imaging results, and complications were recorded and analyzed.

Results: Ten cases averaging 12.90 years of age participated in this study. There were five femur and five tibia reconstructions. The mean follow-up period was 16.90 months. At last follow-up, all patients were alive without tumor recurrence. Average MSTS functional score was 80.33 ± 11.05%. All prostheses were intact and stable without failure or systemic breakage. No serious complications occurred after the operation. Postoperative X-ray, computed tomography (CT) and single-photon emission computed tomography (SPECT) showed an ideal integration between the bone and the prosthetic composite. Moreover, vascularized fibula and implanted β-TCP bioceramics indicated relatively high metabolic activity *in vivo*.

Conclusions: Patient-specific 3D-printed prostheses combined with β-TCP bioceramics and/or vascularized fibula provide an excellent option for reconstruction of massive bone defects after lower extremity malignant tumor extirpation. Short-term follow up showed promising clinical results in recovering lower limb function, promoting osseointegration and reducing complications.

1. Introduction

Limb salvage surgery has become the optimal choice for most malignant tumors of the extremities, due to early diagnosis, neoadjuvant chemotherapy, as well as advances in surgical techniques and medical device industry [1,2]. However, reconstruction of massive bone defects after tumor resection poses a major challenge for surgeons. The traditional options for reconstruction include allografts [3], autografts [4], recycled tumor bone implantation [5] and segmental prosthesis [6,7]. Unfortunately, no standardized method with definite long-term efficacy, reduced complications and excellent postoperative limb functions has been established.

Recently, advanced 3D printing technology has revolutionized the conventional concepts of oncological surgery and made it possible to accurately remove tumors and perform patient-specific reconstruction. In addition to anatomical models and surgical guides, 3D-printed prostheses have been approved for clinical trials and achieved certain success [8–10]. The contour of a 3D-printed

Abbreviations:: β-TCP, beta-tricalcium phosphate; MSTS, Musculoskeletal Tumor Society score; CT, computed tomography; SPECT, single-photon emission computed tomography; SLM, selective laser melting

☆ Declarations of interest: none

* Corresponding authors.
E-mail addresses: wangzhen@fmmu.edu.cn (Z. Wang), 13359265058@189.cn (J. Li).

https://doi.org/10.1016/j.jbo.2019.100220
Received 20 December 2018; Received in revised form 22 January 2019; Accepted 22 January 2019
Available online 25 January 2019

prosthesis could perfectly fit to the bone defect. Moreover, it could be introduced into be porous for the purpose of conducting bone ingrowth and decrease the modulus, which could help reduce long-term mechanical complications, including loosening and fracture [11]. However, the porous metal titanium alloy is, after all, a metallic material which is not biologically active *in vivo*, and several studies have shown that the depth of bone tissue growing into porous metals is limited.

The concept of '*in vivo* osteo-regenerator' was proposed by our research group in 2015, describing the prototype of 3D printed prosthetic composites [12]. Currently, we have developed a novel composite consisting of patient-specific 3D-printed prosthesis, artificial bone materials (β-TCP) and/or vascularized fibula for massive bone defects after wide removal of malignant bone tumors of lower extremities. In this prospective study, we aimed to demonstrate the feasibility of such prosthesis composite and evaluate its short-term clinical efficacy.

2. Materials and methods

2.1. Patients

A prospective study was performed form Jun 2015 to Nov 2018 in the Department of Bone Oncology, Xijing Hospital. Patients meeting the following criteria were included: (1) pathological diagnosis of primary malignant tumor of lower extremities; (2) condition of limb salvage surgery; (3) expected survival time of at least 12 months; (4) voluntarily acceptance of the novel reconstruction material. Patients meeting any of the following criteria were excluded: (1) multiple metastases or unresectable tumors; (2) cardiopulmonary insufficiency, or other serious diseases; (3) pregnancy or lactation in women. The study protocol and interventions were approved by the Clinical Research Ethics Committee of Xijing Hospital, and all participants provided signed informed consent.

2.2. 3D-printed prosthesis

The limbs were scanned by CT (Mutislice 64, GE Healthcare, USA) with the following parameters: slice thickness, 0.625 mm; matrix, 512 × 512; pixel size, 0.2–0.4 mm; feed per rotation, 1 mm. Image data were recorded in DICOM format and imported into the Mimics V17.0 software (Materialise, Belgium) for reconstructing 3D geometric models. MRI images were also obtained to identify tumor margins and reaction areas. Under virtual conditions, the tumor was simulated to be excised with safe margin, with the prosthesis fixed at the defect site. The customized guide plate for osteotomy was designed based on bone surface characteristics and the osteotomy plane. Because tumor invasion usually destroys the structures of affected bones partially or totally, 3D bone models appeared to be incomplete and not suitable for prosthesis design. Therefore, the prosthesis is developed through the mirror image of 3D reconstruction of the unaffected side to ensure the same morphological characteristics. Basically, it is a hollow cylinder, and the bone grafting window is reserved to facilitate the implantation of vascularized fibula and bioceramic granules (Fig. 1A). Osteosynthesis plates were integrated into the prosthesis ends with screw holes, through which the prosthesis can be rigidly fixed onto the host bone. It should be emphasized that except for osteosynthesis plates and the regions requiring mechanical reinforcement, the rest of the prosthesis has a 'super porous interface' structure, which is similar to the three-dimensional structure in natural bone tissue. This structure plays an active role in promoting trabecular ingrowth and enhancing the long-term stability of prosthesis [13,14]. Then, to maintain keen stability, some cylinder holes were designed on the surface of the proximal part of tibial component to attach collateral ligaments. Before processing, the mechanical properties of the designed prosthesis were verified by three-dimensional finite element analysis. Only those that met the mechanical requirements can be transferred to the next step. The 3D printed prosthesis was made of titanium alloy (Ti6Al4V) by the selective laser melting (SLM) technology, and fabricated at Xi'an Bright Laser Technology Co., Ltd. (Xi'an, China). Before clinical application, the prosthesis underwent post-processing of thermal treatment, powder removal, cleaning and sterilization, sequentially.

2.3. Bioceramic granules

The β-TCP porous bioceramics were designed and produced by Shanghai Bio-lu Biomaterials Co, Ltd. (Shanghai, China). In this study, irregular porous bioceramic granules with a diameter of 1.5–3.5 mm were used, which have pore with a diameter of 500–600 μm and the interconnection with a diameter of 120 μm (Fig. 1B, C). β-TCP bioceramics with this specific micro three-dimensional structure has been proved to have the ability to induce angiogenesis and promote osteogenesis during bone defect repairing [15–17]. Moreover, it is biodegradable and finally replaced by the surrounding bone tissue.

2.4. Surgical technique

The most critical steps of the surgical procedure were tumor resection and composite graft installation (Fig. 2). All operations were performed by the same surgical team using standard procedures. With the help of the guide plate, en-bloc resection of the tumor was precisely performed under the principles of tumor-free surgery (Fig. 2B). The reconstruction procedures can be classified into two types, including '3D-printed prosthesis + vascularized fibula + bioceramic granules' (P-F-B) and '3D-printed prosthesis + bioceramic granules'(P-B), based on preoperative design and the patients' wishes (Figs. 3 and 4). Generally, P-B reconstruction was recommended for children below 10 years of age (Fig. 4). For the P-F-B composite, the vascularized fibula was assembled in the center cavity of the 3D printed prosthesis, surrounded by sufficient amounts of bioceramic granules (Fig. 1D). For the P-B composite, the inner cavity of the 3D printed prosthesis was filled with bioceramic granules without fibula (Fig. 4D, E). Furthermore, two different types of vascularized fibula were used for P-F-B reconstruction. For tumors occurring in the tibia and not involving the ipsilateral fibula, the ipsilateral pedicle's vascularized fibula was adopted without vascular anastomosis. For tumors occurring in the femur, a free fibula flap was selected. Peroneal vessels were identified, ligated proximally or distally, and anastomosed to anterolateral thigh vessels under a microscope. Considering the stability of installation, additional plates were used to enhance fixation when necessary. The defective fibula was reconstructed with allograft or 3D-printed fibula (Fig. 2F). For reconstruction around the knee joint, collateral and patellar ligaments were sutured to the reserved cylinder holes on the prosthesis surface. After irrigation with hydrogen peroxide and physiological saline, the incision was sutured layer by layer, and drainage tubes were placed.

2.5. Postoperative management

The patients were advised to stay in bed postoperatively for 6 weeks, during which active and passive joint motion exercises were encouraged. Non-weight-bearing standing and walking were allowed from 6 weeks to 3 months after operation. Partial weight-bearing was encouraged from 3 months post-operation, followed by gradual full weight-bearing based on radiological follow-up results. Radiotherapy, chemotherapy or other medical interventions were allowed when necessary after surgery.

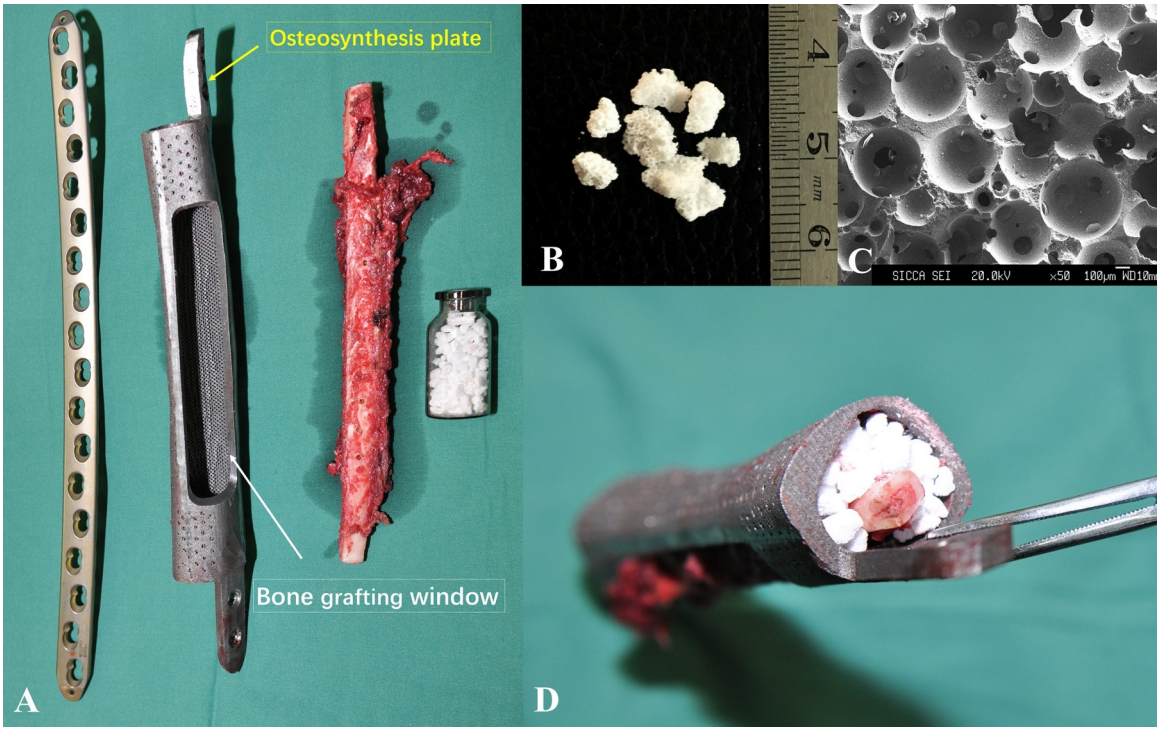

Fig. 1. The implants used in surgery.
A: The implanting system included 3D-printed prosthesis, vascularized fibula, bioceramic granules, and plates.
B: β-TCP bioceramics granules (irregular, with a diameter of 1.5–3.5 mm).
C: Microstructure of the β-TCP bioceramics granules (the pore with a diameter of 500–600 μm and the interconnection with a diameter of 120 μm).
D: Composite (consisted of 3D-printed prosthesis, β-TCP bioceramics granules and vascularized fibula).

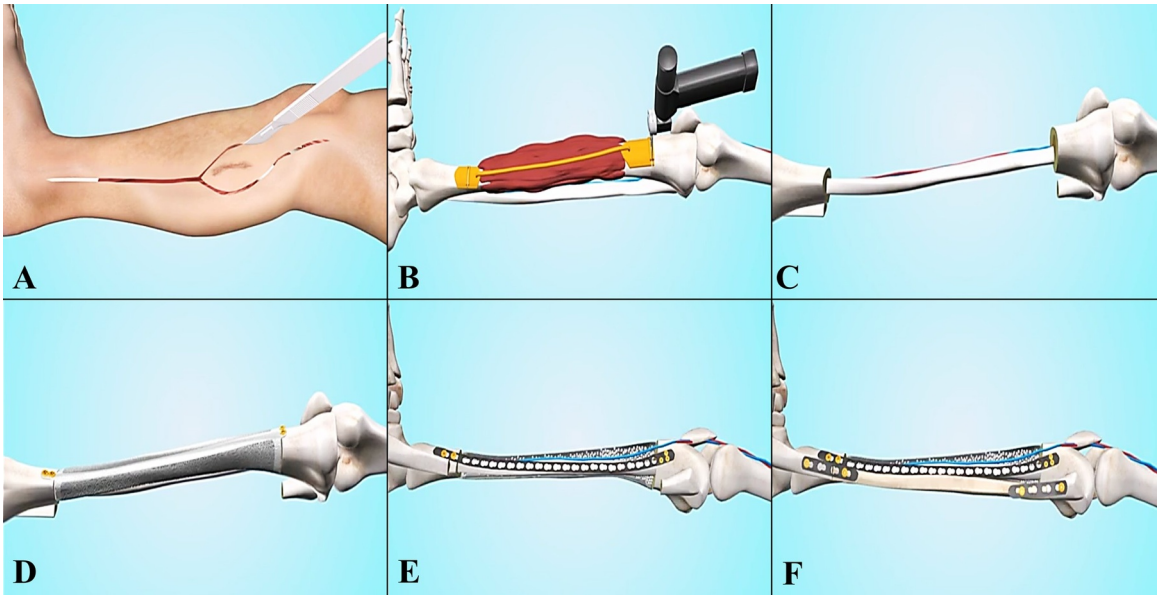

Fig. 2. The main surgical procedures.
A: The design of surgical incision.
B: Tumor resection under surgical guide plate.
C: Vascularized fibula transfer.
D: Installation of the 3D-printed prosthesis.
E: Prosthesis fixation and filling β-TCP bioceramic granules into the cavity of prosthesis.
F: Reconstruction of the defective fibula with allograft bone or 3D-printed titanium fibula.

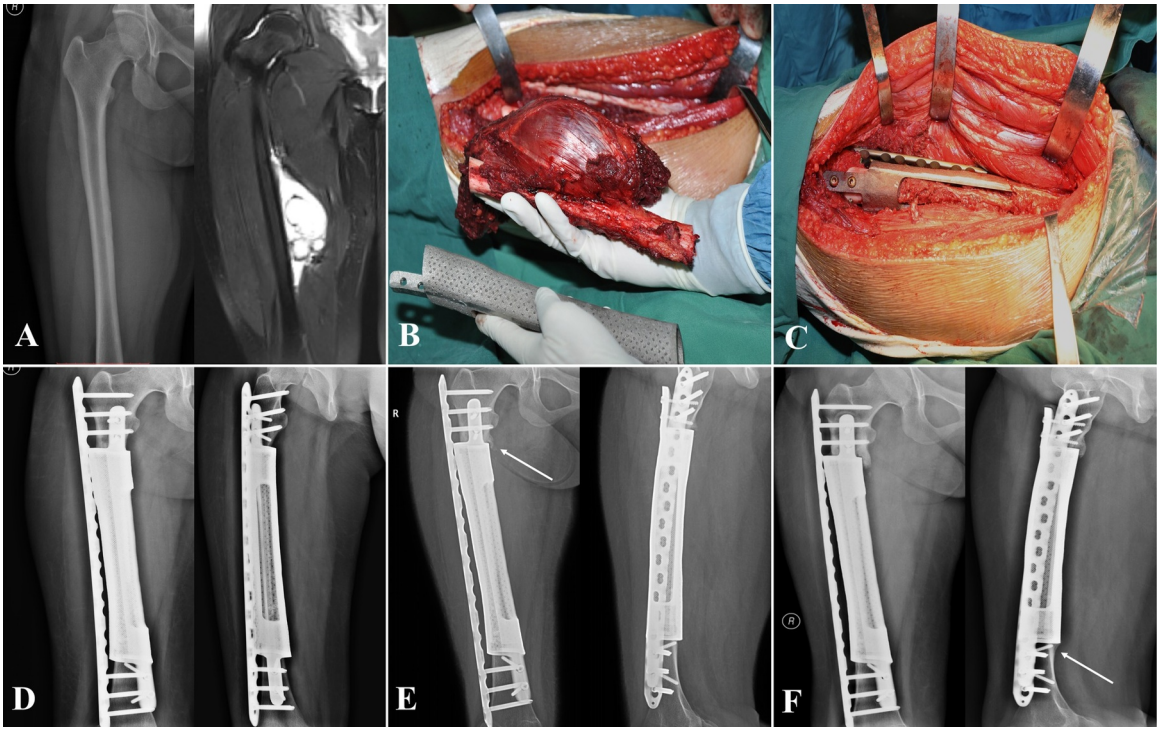

Fig. 3. Case, female, 16 years old, pathological diagnosis of Ewing's sarcoma of the right femur, underwent P-F-B reconstruction.
A: Preoperative X-ray and MRI, showing a huge tumor with a length of 15.13 cm.
B: Tumor resection, the 3D-printed prosthesis perfectly matched the anatomical characteristics of the bone defect.
C: Installation and fixation of the bioactive prosthesis composite.
D: X-ray: one month after operation.
E: X-ray: 12 months after operation, the prosthesis was in situ without loosening. The arrow showed osseous coverage between prosthesis and residual bone.
F: X-ray: 24 months after operation, a solid integration was formed between bone and prosthesis. The arrow indicated a 'spot welding', which connecting edge of the prosthesis to bone.

2.6. Assessment

The patients were followed up clinically and radiologically at 1, 3 and 6 months, and every 3 months thereafter. Anteroposterior and lateral radiographs were used as the basic tools for prosthesis evaluation. Moreover, pulmonary CT was used to assess metastasis; SPECT/CT was recommended for biological evaluation of vascularized fibula and bioceramics. Failure of the prosthesis was evaluated according to the Classification of Segmental Endoprosthetic Failure [18]. The functional outcome of the reconstructed limb was assessed using the MSTS scoring system [19]. Oncological outcomes and complications of the prosthesis were recorded in detail.

2.7. Statistical analysis

All statistical analyses were conducted using SPSS software (version 18.0, Inc., Chicago, Illinois). The quantitative data was described as the mean ± standard deviations (SD). In the comparison between the P-F-B and P-B reconstructions, two-sample *t* tests and *chi-square* tests were used and *p* value less than 0.05 was considered as statistical difference.

3. Results

Patient demographics and treatment data are summarized in Table 1. Ten patients (seven females and three males) fulfilling the inclusion criteria were assessed. Their ages at the time of surgery ranged from 6 to 20 years, with an average of 12.90 years. Of the ten cases, five underwent tumor resection and reconstruction with P-F-B and the remaining five with P-B. Osteosarcoma (7 cases) constituted the most common pathological type among cases. The affected bone sites included proximal femur ($n = 1$), middle femur ($n = 2$), distal femur ($n = 2$), proximal tibia ($n = 3$), middle tibia ($n = 1$) and distal tibia ($n = 1$). Preoperative neoadjuvant chemotherapy was applied to patients with Ewing's sarcoma or osteosarcoma. According to the surgical staging system proposed by Enneking et al., all patients had stage IIB disease.

The average operation time was 218.20 ± 96.37 min (80–385 min), for an average blood loss of 372.00 ± 217.71 ml (100–800 ml). The length of segmental bone defect caused by tumor resection averaged 19.97 ± 6.77 cm (7.06–29.01 cm). The follow-up period after surgery ranged from 5 to 34 months, with an average of 16.90 months.

3.1. Oncological outcomes

At final follow-up, all the patients were alive without tumor recurrence. There was no evidence of disease in 8 of the 10 (80%) patients. Lung metastasis occurred in one patient with osteosarcoma at 16 months after surgery, and resection was performed in the department of thoracic surgery. Another patient with Ewing's sarcoma developed inguinal lymph node metastasis at 12 months postoperatively, and no new lesions were found after radiotherapy.

3.2. Physical function

The average MSTS functional score was 80.33 ± 11.05% (60.00–96.67%) at last follow-up. Patients who underwent femoral and tibial reconstructions scored 74.67 ± 10.16% (60.00–86.67%)

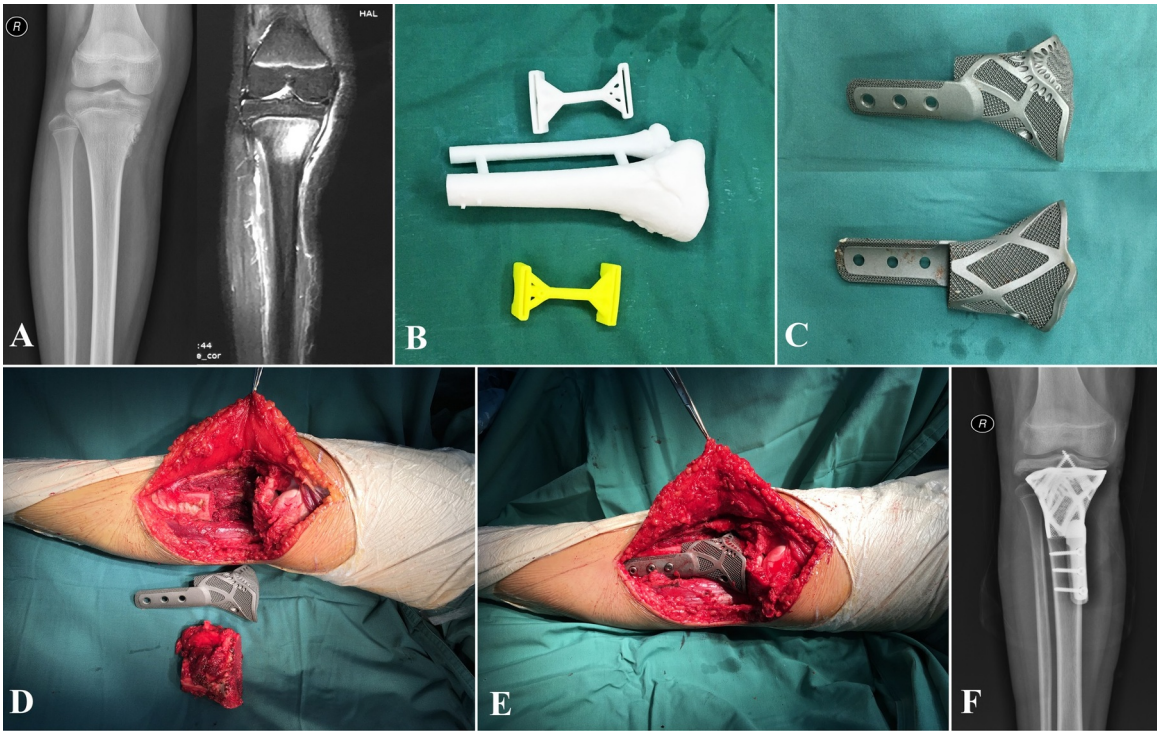

Fig. 4. Case, female, 13 years old, pathological diagnosis of osteosarcoma of the right tibia, underwent P-B reconstruction.
A: Preoperative X-ray and MRI.
B: 3D printed tumor model and osteotomy guide plate.
C: Patient-specific 3D printed prosthesis.
D: Resected tumors, bone defects, and the 3-D printed prosthesis.
E: The contour of 3D-printed prosthesis perfectly match to the bone defect.
F: X-ray: One month after operation.

and 86.00 ± 9.55% (73.33–96.67%), respectively, indicating a non-statistically significant difference ($p = 0.107$). Six patients with MSTS scores ≥80% were able to carry out normal activities and work. There was only one patient with a score ≤60%.

3.3. Prosthesis evaluation

All reconstructs were in situ during the follow up period (Figs. 3 and 4). According to the Classification of Segmental Endoprosthetic Failure, no soft-tissue failure, aseptic loosening or structure failure was recorded. Additionally, no non-mechanical failure (infection or tumor progression) was found in these cases. The implants had no issues in 9 of the 10 (90%) patients. Two fixed screws were fractured in one of the ten patients, but did not affect prosthesis stability, so further clinical interventions were not required. The composites resulted in substantial bone integration during follow-up for more than 12 months after the operation, with the following manifestations: (1) osseous coverage formed by the extension of cortical bone to the prosthesis; (2) bone union between the vascularized fibular grafting and residual bone; (3) β-TCP bioceramic granules in the 3D printed prosthetic cavity were partially degraded, accompanied by new bone formation (Fig. 5D, E). Postoperative SPECT/CT demonstrated that all four fibula flaps survived (Fig. 5A). It should be noted that the bioceramics inside the prosthesis cavity also showed relatively high metabolic activity, reflecting the bone formation process (Fig. 5C).

3.4. Postoperative complications

All the operations were successful without intraoperative complications. One patient with pool related wound was cured after several cycles of debridement and wound dressing. No other postoperative complications such as infection, thrombosis, fracture and variable donor-site morbidity occurred in this case series during follow-up.

3.5. P-F-B versus P-B

According to reconstruction methods, the cases could be further divided into two subgroups, including A and B, who received reconstructions with P-F-B and P-B, respectively. There were no statistically significant differences in gender and Enneking stage between the two groups ($p = 0.490$). However, age in group B was reduced compared with that of group A (9.80 ± 2.77 y versus 16.00 ± 3.94 y, $p = 0.021$). Bone defect lengths in groups A and B were 24.39 ± 2.82 cm and 15.55 ± 6.81 cm, respectively, indicating a significant difference ($p = 0.028$). Mean operation time in group A was 298.40 ± 49.65 min, which was significantly longer than that of group B (138.00 ± 48.55 min, $p = 0.000$). Moreover, group A had more intraoperative blood loss than group B (504.00 ± 187.29 ml versus 240.00 ± 167.33 ml, $p = 0.046$). At final follow-up, all prostheses in groups A and B were in situ, and no prosthesis failures such as loosening, infection and fracture were found. In terms of limb function, average MSTS scores in groups A and B were 80.00 ± 7.07% and 80.67 ± 14.68%, respectively, with no statistically significant difference ($p = 0.931$). The detailed information is shown in Table 2.

Table 1
Clinical features and follow-up results of the patients.

No.	Gender	Age	Diagnosis	Site	Enneking Stage	Length of bone resected (cm)	Reconstruction	Operation time (min)	Intraoperative bleeding (ml)	Follow-up (mo)	Oncological outcome	MSTS score
1	male	15	Ewing's sarcoma	Left femur(middle)	II B	29.01	P-F-B	282	520	12	NED	86.67%
2	female	20	Chondrosarcoma	Left femur(distal)	II B	24.71	P-F-B	275	400	24	NED	76.67%
3	female	16	Ewing's sarcoma	Right femur(middle)	II B	22.05	P-F-B	385	800	34	Lymph node metastasis; NER	80.00%
4	female	19	Osteosarcoma	Left tibia(middle)	II B	22.23	P-F-B	260	500	27	Lung metastasis; NER	86.67%
5	male	10	Osteosarcoma	Left femur(distal)	II B	23.94	P-F-B	290	300	17	NED	70.00%
6	female	6	Osteosarcoma	Left tibia(proximal)	II B	13.44	P-B	175	100	13	NED	96.67%
7	female	9	Osteosarcoma	Left tibia(distal)	II B	19.94	P-B	80	100	10	NED	93.33%
8	male	9	Osteosarcoma	Right tibia (proximal)	II B	24.6	P-B	140	300	14	NED	80.00%
9	female	12	Osteosarcoma	Left femur (proximal)	II B	12.71	P-B	195	500	13	NED	60.00%
10	female	13	Osteosarcoma	Right tibia (proximal)	II B	7.06	P-B	100	200	5	NED	73.33%

Notes: P-F-B = 3D-printed prosthesis + vascularized fibula + bioceramic granules; P-B = 3D-printed prosthesis + bioceramic granules; NED = no evidence of disease, NER = no evidence of recurrence.

4. Discussion

In this study, we developed a novel prosthesis composite under guidance of the '*in vivo* osteo-regenerator' concept, which was put forward and verified in animal experiments [12]. The regenerator was designed to use the body itself as a reactor to generate the required bone tissue with the help of bioactive scaffolds. Preferably, β-TCP granules were selected as scaffolds because of favorable biocompatibility, osteoconductivity, biodegradability and angiogenesis inducibility [15–17,20,21]. For reconstruction in this study, the soft tissue around the prosthesis and truncation surface of the bone and/or vascularized fibula in the prosthetic cavity constituted the biological environment of the regenerator. β-TCP granules in the prosthetic cavity played the role of biological conduction, through which osteogenesis progressed along with the degradation of bioceramics.

Satisfactory tumor-negative margins were achieved in all ten patients, and bone defects were successfully reconstructed. As clinical results, postoperative MSTS scores at final follow-up averaged 80.33 ± 11.05%, comparable with the results of segmental prostheses in other publications [22–24]. Yan et al.[22] reported 30 cases who underwent wide excision and reconstruction using tumor endoprosthesis; mean MSTS scores for proximal femur, distal femur, proximal tibia, proximal humerus, and total femur were 90%, 82%, 73%, 71% and 60%, respectively. In a study by Holm et al. [23], 50 patients with primary bone tumors of lower extremities who underwent limb-sparing reconstruction with mega-prostheses were followed up for a mean of 14 years. The mean MSTS score of 24 patients whose limbs were still spared at last follow-up was 21.2 (range 6–30), representing a median score of 71%.

Soft tissue failure, aseptic loosening, structural failure, infection, and tumor progression are the five common complications that lead to failure of tumor endoprostheses [18]. Kawai et al. [25] reported that aseptic loosening is the primary cause of prosthetic failure. In this study, we did not observe infection, aseptic loosening, soft-tissue failure, prosthesis breakage or tumor recurrence. This is partly because the bioactive 3D-printed prosthesis composite combines the advantages of immediate mechanical endurance of a porous titanium prosthesis and the long-standing biological properties of β-TCP bioceramics and/or a vascularized fibula graft. However, long-term complications need to be further assessed since some of them usually arise 2 years after operation [26]. Compared with traditional segmental prosthesis, the 3D printed prosthetic composite has the advantages of biocompatibility, bioactivity, and biological stability, which can reduce the incidence of complications and achieve better long-term efficacy theoretically.

The Young's modulus of titanium (110 Gpa) is several times greater than that of cortical bone (7–30 Gpa), which creates a stress-shielding effect and eventually leads to bone resorption and prosthetic failure [27]. It was reported that the mechanical properties of 3D-printed prostheses with mesh or porous structure are more suitable than those of conventional solid prostheses [25,28]. In this study, the mechanical structures of 3D printed prostheses were optimized by topological methods and tested by three-dimensional finite element analysis. This is obviously different from traditional prostheses in that the mechanical properties of the 3D printed prosthetic composite are gradually enhanced due to bone formation promoted by β-TCP bioceramics inside the prosthesis. Benefiting from these excellent mechanical properties, all patients could achieve partial weight-bearing walk at 3 months after surgery, and no breakage or loosening of the prosthesis was found during clinical follow-up.

Vascularized fibula transfer is considered an adequate method for limb sparing surgery since it was first described in the late 1970s [29]. Vascularized fibula flaps are mainly used in intercalary reconstruction of upper limbs, and bony union is achieved in the majority of cases [30,31]. However, for reconstructing lower limb

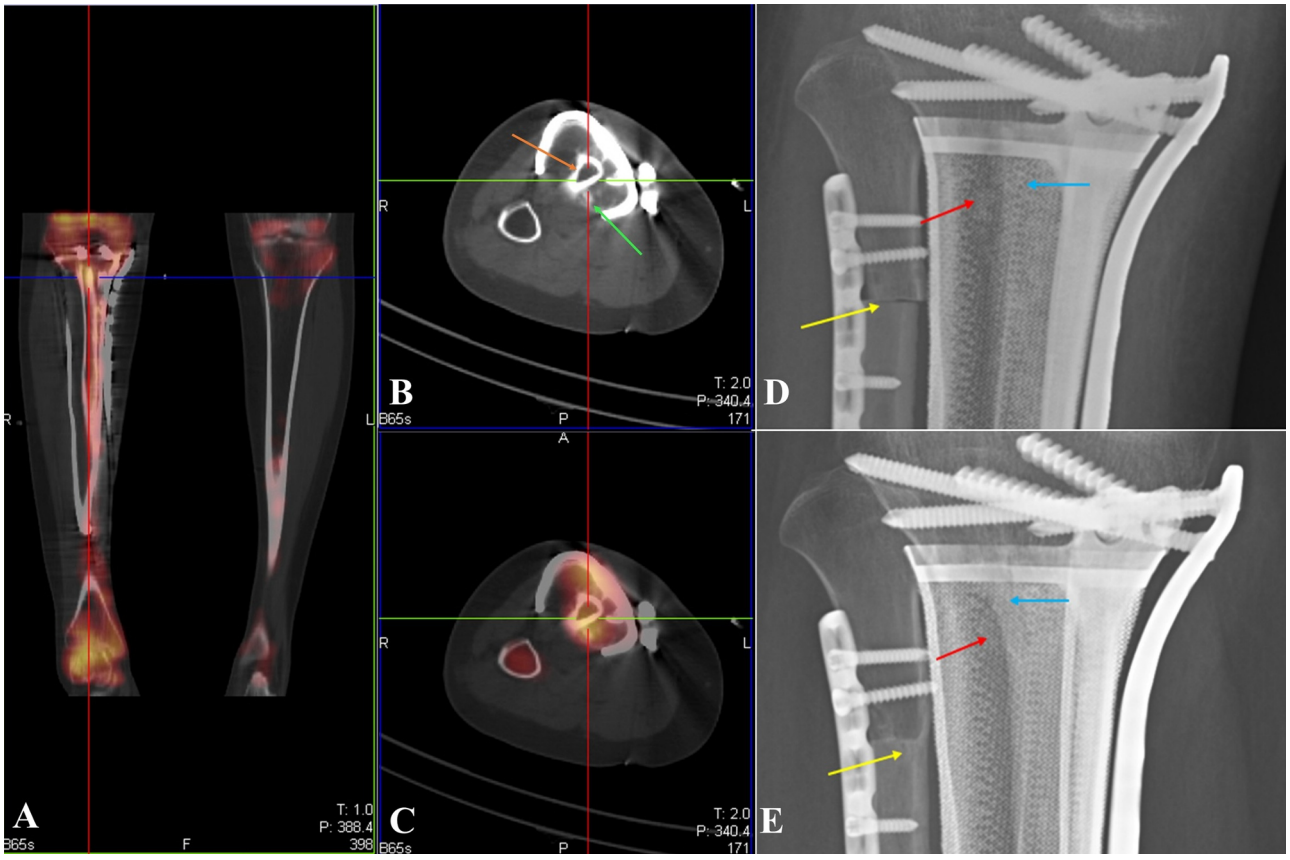

Fig. 5. The evaluation of bioceramics and vascularized fibula.
A: SPECT (Coronal position) showed the fibula flaps were survived.
B: CT (Axial position), the orange arrow orange indicated the vascularized fibula; the green arrow indicated the β-TCP bioceramic granules.
C: SPECT/CT (Axial position), showing high metabolic activities in the vascularized fibula and the surrounding *β*-TCP bioceramic granucles.
D: X-ray: one week after operation, the initial position of the vascularized fibula (the blue arrow), bioceramic granules (the red arrow) and allograft fibula (the yellow arrow).
E: X-ray: 21 months after operation, 'umbrella like' bone formation was observed at the end of the vascularized fibula (the blue arrow); bioceramic granules were degraded for new bone formation (red arrow); the allograft fibula and the remaining bone were linked together (red arrow). (For interpretation of the references to colour in this figure legend, the reader is referred to the web version of this article.)

Table 2
The comparison between the reconstruction with P-F-B and P-B.

	Group A (with P-F-B)	Group B (with P-B)	*P* value
The baseline data of patients			
Gender (female/male)	3/2	4/1	0.490
Age (SD)/year *	16.00(3.94)	9.80(2.77)	0.021
Enneking Stage	II B (5 cases)	II B (5 cases)	
Surgical operation			
Length of bone resected (SD)/cm *	24.39(2.82)	15.55(6.81)	0.028
Operation time (SD)/min *	298.40(49.65)	138.00(48.55)	0.000
Intraoperative bleeding (SD)/ml *	504.00(187.29)	240.00(167.33)	0.046
Functional outcome			
MSTS score (SD)/(%)	80.00% (7.07%)	80.67% (14.98%)	0.931

* Differences between the two groups were statistically significant.

bone defects, the mechanical strength of the fibula is insufficient. Patients are usually not allowed to weight-bearing stand or walk for a long period after surgery. Even so, stress fracture of the transferred fibula is a common complication with reported rates ranging between 7.7 and 22.2% [32,33]. To solve this problem, the Capanna technique that combines a large structural allograft with a free fibular flap is an alternative [34]. However, this method incorporates the dual complications of allografts and autologous fibular grafts, such as nonunion, infection, pathophoresis and donor-site discomfort. In the current series, four cases with femur malignancy and one with tibia malignancy were reconstructed using 3D printed prosthesis combined with vascularized fibula and *β*-TCP bioceramics. Patient-specific prostheses provide early mechanical stability, and the vascularized fibula and bioceramics inside the prosthesis substantially improve the biological properties of the reconstruction. During follow-up, bone union was achieved in all cases. However, it should be noted that fibula transplantation is not highly recommended for younger children because of thin fibula, and the absence of fibula may affect the skeletal development of lower extremities [35]. In addition, it is associated with variable donor-site complications, including motor weakness, pain and sensory abnormalities [36,37]. Therefore, P-B composite reconstruction without vascularized fibula was adopted for five children in this study. The biological properties and bone regeneration ability of bioceramic granules inside the prosthesis are the most important concerns. As a bone substitute material, *β*-TCP provides osteoconductive activity and is biodegradable. In a previous study

[38], β-TCP was used to backfill the fibular defect caused by bone harvesting. Callus formation bridging the beta-TCP was recorded at an early stage after operation, and the β-TCP mostly was absorbed and replaced by newly formed bone at an average of 9.3 months postoperatively. Moreover, the vascular conductivity and angiogenic activity of β-TCP bioceramics with specific pore structure have been confirmed, and the bioceramics rod has been used to reestablish blood supply upon femoral head necrosis [39]. In P-B reconstruction, cells and fluids abundantly flow into the β-TCP bioceramics granules through the medullary cavity and the superporous structure of the 3D printed prosthesis; eventually, the internal part of the prosthesis is replaced by the mature new bone, which improves the permanent stability of the reconstruction. Compared with P-F-B reconstruction, the P-B procedure takes less time ($p = 0.000$) and causes reduced intraoperative blood loss ($p = 0.046$). As short-term results, the MSTS score of P-B reconstruction was 80.67% ± 14.98%, which was not statistically different from that of P-F-B reconstruction (80.00% ± 7.07%, $p = 0.931$). It can be further hypothesized that there is no difference in clinical efficacy for β-TCP bioceramics/3D printed prosthesis composite with or without fibula, and P-B reconstruction can also be applied to adults. However, limited by short follow-up time, this remains to be further investigated.

5. Conclusions

To conclude, these preliminary results revealed that the novel composite offers promising clinical outcomes. With vascularized fibula and bioceramics, the risk of complications and failure seems to be reduced. Use of the 3D-printed prosthesis in combination with β-TCP bioceramics and/or vascularized fibula represents an attractive option for reconstructing large bone defects after tumor resection. However, we acknowledge the limitations of this study. Firstly, short-term follow-up was the major limitation. Another shortcoming was the lack of a control group, which limited statistical power. Additionally, this technique has a short duration of use, and the sample size was relatively small. Therefore, multi-center controlled studies are required to adequately evaluate the clinical efficacy of this new technique in long term follow-up.

Conflict of interest statement

There is no financial support or other benefits and no commercial sources for the work. The authors declare that there are no conflicts of interest.

Supplementary material

Supplementary material associated with this article can be found, in the online version, at doi:10.1016/j.jbo.2019.100220.

References

[1] A.F. Kamal, H. Widyawarman, K. Husodo, et al., Clinical outcome and survival of osteosarcoma patients in cipto Mangunkusumo hospital: limb salvage surgery versus amputation, Acta Medica Indonesiana 48 (2016) 175–183.

[2] G. Ottaviani, R.S. Robert, W.W. Huh, et al., Functional, psychosocial and professional outcomes in long-term survivors of lower-extremity osteosarcomas: amputation versus Limb salvage, Cancer Treat. Res. 152 (2009) 421–436.

[3] H.N. Shih, Y.J. Chen, T.J Huang, et al., Semi structural allografting in bone defects after curettage, J. Surg. Oncol. 68 (2015) 159–165.

[4] T.A. Russell, R.K. Leighton, Comparison of autogenous bone graft and endothermic calcium phosphate cement for defect augmentation in tibial plateau fractures. A multicenter, prospective, randomized study, J. Bone Joint Surg. AM 90 (2008) 2057–2061.

[5] X.C. Yu, M. Xu, S.F. Xu, et al., Long-term outcomes of epiphyseal preservation and reconstruction with inactivated bone for distal femoral osteosarcoma of children, Othop. Surg. 4 (2012) 21–27.

[6] G.W. Blunn, T.W. Briggs, S.R. Cannon, et al., Cementless fixation for primary segmental bone tumor endoprostheses, Clin. Orthop. Relat. Res. 372 (2000) 223–230.

[7] E.Y. Chao, B. Fuchs, C.M. Rowland, et al., Long-term results of segmental prosthesis fixation by extracortical bone-bridging and ingrowth, J. Bone Joint Surg. AM 86 (2004) 948–955.

[8] S. Arabnejad, B. Johnston, M. Tanzer, et al., Fully porous 3D printed titanium femoral stem to reduce stress-shielding following total hip arthroplasty, J. Orthop. Res. 35 (2017) 1774–1783.

[9] H. Liang, T. Ji, Y. Zhang, et al., Reconstruction with 3D-printed pelvic endoprostheses after resection of a pelvic tumour, Bone Joint J. 99 (2017) 267–275.

[10] H. Fan, J. Fu, X. Li, et al., Implantation of customized 3-D printed titanium prosthesis in limb salvage surgery: a case series and review of the literature, World J. Surg. Oncol. 13 (2015) 308.

[11] F.A. Shah, O. Omar, F. Suska, et al., Long-term osseointegration of 3D printed CoCr constructs with an interconnected open-pore architecture prepared by electron beam melting, Acta Biomater. 36 (2016) 296–309.

[12] P. Gao, H. Zhang, Y. Liu, et al., Beta-tricalcium phosphate granules improve osteogenesis in vitro and establish innovative osteo-regenerators for bone tissue engineering *in vivo*, Sci. Rep. 6 (2016) 23367.

[13] X. Wang, S. Xu, S. Zhou, et al., Topological design and additive manufacturing of porous metals for bone scaffolds and orthopaedic implants: a review, Biomaterials 83 (2016) 127–141.

[14] N. Taniguchi, S. Fujibayashi, M.K. Takemoto, et al., Effect of pore size on bone ingrowth into porous titanium implants fabricated by additive manufacturing: an *in vivo* experiment, Mater. Sci. Eng. C. 59 (2016) 690e701.

[15] B. Feng, Z. Jinkang, W. Zhen, et al., The effect of pore size on tissue ingrowth and neovascularization in porous bioceramics of controlled architecture *in vivo*, Biomed. Mater. 6 (2011) 15007.

[16] X. Xiao, W. Wang, D. Liu, et al., The promotion of angiogenesis induced by three-dimensional porous beta-tricalcium phosphate scaffold with different interconnection sizes via activation of PI3K/Akt pathways, Sci. Rep. 5 (2015) 9409.

[17] S. Xu, K. Lin, Z. Wang, et al., Reconstruction of calvarial defect of rabbits using porous calcium silicate bioactive ceramics, Biomaterials 29 (2008) 2588–2596.

[18] E.R. Henderson, J.S. Groundland, E. Pala, et al., Failure mode classification for tumor endoprostheses: retrospective review of five institutions and a literature review, J. Bone Joint Surg. AM 93 (2011) 418–429.

[19] W.F. Enneking, W. Dunham, M.C. Gebhardt, et al., A system for the functional evaluation of reconstructive procedures after surgical treatment of tumors of the musculoskeletal system, Clin. Orthop. Relat. Res. 286 (1993) 241–246.

[20] X. Guo, C. Wang, Y. Zhang, et al., Repair of large articular cartilage defects with implants of autologous mesenchymal stem cells seeded into beta-tricalcium phosphate in a sheep model, Tissue Eng. 10 (2004) 1818–1829.

[21] M. Zhang, K. Wang, Z. Shi, et al., Osteogenesis of the construct combined BMSCs with beta-TCP in rat, J. Plast. Reconstr. Aesthet. Surg. 63 (2010) 227–232.

[22] T.Q. Yan, W.H. Zhou, W. Guo, et al., Endoprosthetic reconstruction for large extremity soft-tissue sarcoma with juxta-articular bone involvement: functional and survival outcome, J. Surg. Res. 187 (2014) 142–149.

[23] C.E. Holm, C. Bardram, A.F. Riecke, et al., Implant and limb survival after resection of primary bone tumors of the lower extremities and reconstruction with megaprostheses fifty patients followed for a mean of forteen years, Int. Orthop. 42 (2018) 1175–1181.

[24] T. Kostuj, R. Streit, M.H. Baums, et al., Midterm Outcome after mega-prosthesis implanted in patients with bony defects in cases of revision compared to patients with malignant tumors, J. Arthroplasty 30 (2015) 1592–1596.

[25] A. Kawai, P.P. Lin, P.J. Boland, et al., Relationship between magnitude of resection, complication, and prosthetic survival after prosthetic knee reconstructions for distal femoral tumors, J. Surg. Oncol. 70 (2015) 109–115.

[26] Y.J. van Slooten, H.G Freling, J.P. van Melle, et al., Long-term tricuspid valve prosthesis-related complications in patients with congenital heart disease, Eur. J. Cardiothorac. Surg. 45 (2014) 83–89.

[27] M. Dewidar, H.F. Mohamed, J.K. Lim, A new approach for manufacturing a high porosity Ti-6Al-4V scaffolds for biomedical applications, J. Mater. Sci. Technol. 24 (2008) 931–935.

[28] L. Xiang, C. Wang, W. Zhang, et al., Fabrication and characterization of porous Ti6Al4V parts for biomedical applications using electron beam melting process, Matter. Lett. 63 (2009) 403–405.

[29] G.I. Taylor, G.D. Miller, F.J. Ham, The free vascularized bone graft. A clinical extension of microvascular techniques, Plast. Reconstr. Surg. 55 (1975) 533–544.

[30] M. Gerwin, A.J. Weiland, Vascularized bone grafts to the upper extremity: indications and technique, Microsurgery 8 (1992) 509–523.

[31] H. Yijima, S. Tamai, H. Ono, et al., Vascularized bone grafts to the upper extremities, Plast. Reconstr. Surg. 101 (1998) 727–737.

[32] K. Ihara, K. Doi, M. Yamamoto, S. Kawai, Free vascularized fibular grafts for large bone defects in the extremities after tumour excision, J. Reconstr. Microsurg. 14 (1998) 371–376.

[33] S.N. Amr, A.O. El-Mofty, S.N. Amin, A.M. Morsy, O.M. El-Malt, H.A. AbdelAal, Reconstruction after resection of tumours around the knee: role of the free vascularized fibular graft, Microsurgery 20 (2000) 233–251.

[34] R. Capanna, C. Bufalini, C. Campanacci, A new technique for reconstruction of large metadiaphyseal bone defects: a combined graft (allograft shell plus vascularized fibula), Orthop. Traumatol. 2 (1993) 159–161.

[35] P. Gonzálezherranz, R.A. Del, J. Burgos, et al., Valgus deformity after fibular

resection in children, J. Pediatr. Orthop. 24 (2004) 345–346.
[36] A.E. Beris, M.G. Lykissas, A.V. Korompilias, et al., Vascularized fibula transfer for lower limb reconstruction, Microsurgery 31 (2011) 205–211.
[37] H. Yajima, S. Tamai, S. Mizumoto, et al., Vascularized fibula graft for reconstruction after resection of aggressive benign and malignant bone tumors, Microsurgery 13 (2010) 227–233.
[38] E. Arai, H. Nakashima, S. Tsukushi, et al., Regenerating the fibula with beta-tricalcium phosphate minimizes morbidity after fibula resection, Clin. Orthop. Relat. R. 431 (2005) 233–237.
[39] Y. Lu, X. Lu, M. Li, et al., Minimally invasive treatment for osteonecrosis of the femoral head with angioconductive bioceramic rod, Int. Orthop. 42 (2018) (2018) 1–7.